# INCREMENTAL IDENTIFICATION OF TRANSPORT PHENOMENA IN CONVECTION-DIFFUSION SYSTEMS

MAKA KARALASHVILI*, SVEN GROß†, ADEL MHAMDI*, ARNOLD REUSKEN†, AND WOLFGANG MARQUARDT*

**Abstract.** In this paper an incremental approach for the identification of transport phenomena in convection-diffusion systems on the basis of high-resolution measurement data is presented. The transport is represented by a convection term with known convective velocity and by a diffusion term with an unknown, generally state-dependent transport coefficient. The reconstruction of this transport coefficient constitutes an ill-posed nonlinear inverse problem. We present a novel decomposition approach in which this inverse problem is split into a sequence of inverse subproblems. The inverse problems arising in the different identification steps of this incremental approach are solved by means of the conjugate gradient method in which an adjoint problem is solved for gradient computation. The ill-posedness of each inverse problem is examined by using artificially perturbed transient simulation data and appropriate regularization techniques. The identification methodology is illustrated for a three-dimensional convection-diffusion equation that has its origin in the modeling and simulation of energy transport in a laminar wavy film flow.

**Key words.** Modeling, transport phenomena, convection-diffusion equation, inverse problem, regularization, conjugate gradient method, identification.

**AMS subject classifications.** 15A15, 15A09, 15A23

## 1. Introduction.

Let $\Omega \subset \mathbb{R}^3$ be a computational domain, with boundary parts $\partial\Omega = \Gamma_D \cup \Gamma_N$, where the indices $D$ and $N$ indicate the Dirichlet and Neumann parts of the boundary, respectively. We consider a convection-diffusion equation without sources

$$\frac{\partial \rho u}{\partial t} + \nabla \cdot (\rho u \mathbf{w}) - \nabla \cdot (a \nabla u) = 0 \quad \text{in } \Omega \times (t_0, t_f]\,, \tag{1.1a}$$

and with initial and boundary conditions

$$\begin{aligned} u(\mathbf{x}, t_0) &= u_0(\mathbf{x})\,, \quad \mathbf{x} \in \Omega\,, \\ u(\mathbf{x}, t) &= g_D(\mathbf{x}, t)\,, \quad (\mathbf{x}, t) \in \Gamma_D \times [t_0, t_f]\,, \\ \frac{\partial u}{\partial n}(\mathbf{x}, t) &= g_N(\mathbf{x}, t)\,, \quad (\mathbf{x}, t) \in \Gamma_N \times [t_0, t_f]\,. \end{aligned} \tag{1.1b}$$

The scalar state variable $u(\mathbf{x}, t)$ represents, e. g. specific enthalpy in case of energy transport or mass density in case of mass transport. $\rho(\mathbf{x}, t)$ stands for the density of the fluid. The vector field $\mathbf{w}(\mathbf{x}, t) \in \mathbb{R}^3$ represents velocity and is assumed to be known. The scalar function $a(\,\cdot\,)$ denotes the unknown, in general state-dependent, transport coefficient.

The transport coefficient describes complicated transport phenomena, for which on the basis of different assumptions and theories, a multitude of competing candidate model structures can be formulated. Experimental data should be used to estimate parameters that occur in these candidate models and to discriminate between the competing candidate models using some reasonable measure of model validity.

*Process Systems Engineering, RWTH Aachen University, Turmstrasse 46, D-52064 Aachen, Germany ({karalashvili, mhamdi, marquardt}@lpt.rwth-aachen.de).

†Numerical Mathematics, RWTH Aachen University, Templergraben 55, D-52056 Aachen, Germany ({gross, reusken}@igpm.rwth-aachen.de).

The identification of transport coefficients from appropriate measurement data, such as temperature or concentration, belongs to the class of ill-posed inverse problems. Many studies on the estimation of transport coefficients are available. One possible solution technique is the so-called equation error method [9, 16, 24]. In that approach the transient measurement data are inserted in the model (1.1) which is then interpreted as a system of equations for the unknown coefficient, the integration of which results in a direct relationship between the measured data and unknown coefficient values. This relationship is frequently quite complicated and the transport coefficient has to be determined using special problem adapted methods. Thus, equation error methods are rather problem dependent. Another well-established technique for the identification of transport coefficients relies on an optimization-based formulation that is used in the framework of a *coefficient inverse problem*, cf. [2]. In this approach the reconstruction of the transport coefficient in model (1.1) uses suitable transient measurement data $u_m(\mathbf{x}, t)\,, (\mathbf{x}, t) \in \Omega \times [t_0, t_f]$, and often it is assumed that the initial and boundary conditions of the problem are known. Quite some literature is available on the subject (cf. [3, 18, 26] and the references therein); the treatment, however, is typically restricted to one or two space dimensions.

In the so-called *simultaneous* approach, the problem (1.1) for the identification of the transport coefficient is solved for each model candidate using, for example, one of the above mentioned techniques. This leads to a large number of complex estimation problems. As a consequence, the discrimination between competing model candidates requires high computational efforts. Furthermore, if a model candidate for the transport coefficient contains uncertainty or structural errors, this approach often yields biased or very poor estimates [27]. Often satisfactory results can only be achieved if the correct model structure for the transport coefficient is known. In the present work in contrast, we use a fundamentally different so-called *incremental* approach [19] for the identification of the transport coefficient.

In the incremental *modeling* approach the model structure is refined step by step by specifying submodels gradually. This yields more transparency concerning the individual decisions during the modeling process. The incremental *identification* of the transport coefficient reflects the steps of incremental modeling by splitting up the identification problem into a sequence of subproblems. The discrimination between the candidate models turns out to become more flexible as the replacement of a submodel on a certain model refinement level affects only the submodels on the following levels. Often this also leads to benefits in terms of less computational effort. The incremental strategy already proved to be an efficient and robust alternative for the mechanistic modeling of kinetic phenomena [20], the reconstruction of transport coefficients in distributed systems [5] and the identification of complex reaction kinetics in homogeneous systems [7].

In this paper, we present and investigate the incremental method of modeling and identification for the class of inverse transport coefficient problems described above. The application of the incremental approach to this class of problems is new. As a first step in the analysis of this technique, we show based on simulated data corresponding to a given transport coefficient, that this coefficient can be reconstructed without using any a-priori knowledge on the structure of this coefficient. We also show that the method yields satisfactory results if we add noise to the data. These results indicate that the incremental approach is a promising method for this class of transport identification problems, too.

The paper is organized as follows. The incremental approach of modeling and

identification of transport phenomena is presented in Section 2. The optimization-based formulations for the inverse problems arising during the identification process are given in Section 3. In that section we also describe the conjugate gradient solution method based on adjoint problems for gradient computation. In Section 4 we give results of extensive numerical experiments for the transport coefficient identification in a three-dimensional convection-diffusion problem. This model problem is motivated by research on energy transport in wavy films, using effective transport coefficients [6, 9, 28]. Section 5 contains some conclusions and remarks concerning future work.

**2. Incremental modeling and identification.** The key idea of the incremental approach is the gradual refinement of the model structure during identification, reflecting the incremental steps which are common in model development. The main steps of model development and their relation to incremental model identification are outlined in the following.

**2.1. Incremental modeling.** Incremental modeling aims at a generic and structured process for the development of model equations [19, 20]. The starting point is the formulation of the balance equations. The balance equation for the scalar state $u(\mathbf{x}, t)$, which denotes the specific quantity conserved, is given by

$$\frac{\partial \rho u}{\partial t} + \nabla \cdot \mathbf{j} = 0\,.$$

Here, $\mathbf{j}$ is the flux vector, which governs the rate of transfer of the conserved physical quantity. This vector consists of a convective and diffusive part:

$$\mathbf{j} = \rho u \mathbf{w} + \mathbf{q}\,.$$

Using the continuity equation

$$\frac{\partial \rho}{\partial t} + \nabla \cdot \rho \mathbf{w} = 0\,,$$

this leads to the convection-diffusion equation (cf. Fig. 2.1)

$$\text{model } B\text{:} \qquad \frac{\partial u}{\partial t} + \mathbf{w} \cdot \nabla u = -\frac{1}{\rho} \nabla \cdot \mathbf{q} \quad \text{in } \Omega \times (t_0, t_f]\,. \tag{2.1}$$

We do not refine this equation any further, i. e. at this decision level no additional assumptions are made about the potentially uncertain constitutive relation for the diffusive flux vector $\mathbf{q}$.

In the next step, the model is refined by specifying a functional form of the flux $\mathbf{q}$. For this often a constitutive relation is used, for example, Fourier's law in heat transfer or Fick's law in mass transfer. This then yields

$$\text{model } F\text{:} \qquad \mathbf{q} = -a \nabla u \quad \text{in } \Omega \times (t_0, t_f]\,, \tag{2.2}$$

with an unknown transport coefficient $a$. In empirical approaches one usually distinguishes different transport mechanisms, namely transport by turbulent mechanisms and transport by molecular means, with or without convection [8]. Accordingly, the transport coefficient in (2.2) is represented as a sum of two contributions - the *known* molecular part $a_{\mathrm{mol}}$, the *molecular transport coefficient* corresponding to molecular transport (e. g. heat conduction through the fluid) and the *unknown* remaining part $a_w(\mathbf{x}, t)$ capturing the remaining transport effects (e. g. due to turbulence or transport

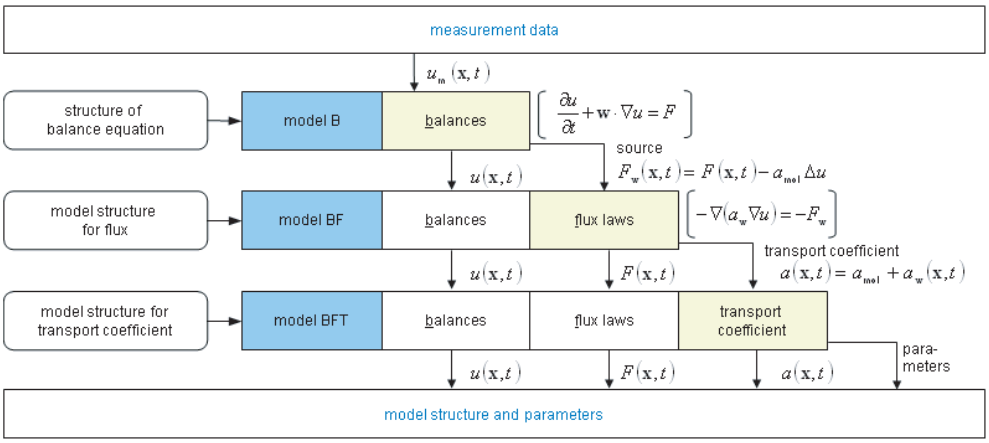


FIG. 2.1. *Incremental modeling and identification of transport phenomena.*

enhancing effects). In the following we call $a_w(\mathbf{x},t)$ the *enhanced transport coefficient*. Thus,

$$a(\mathbf{x},t) = a_{\mathrm{mol}} + a_w(\mathbf{x},t)\,, \quad (\mathbf{x},t) \in \Omega \times [t_0,t_f]\,. \tag{2.3}$$

Consequently the flux law (2.2) can be written as

$$\mathbf{q} = -(a_{\mathrm{mol}} + a_w)\nabla u \quad \text{in } \Omega \times (t_0,t_f]\,. \tag{2.4}$$

In the final step of the incremental modeling, a further refinement level is added by specifying a constitutive relation for the transport coefficient to close the model. Since the functional form of this relation is still unknown, we formulate it in a generic way,

$$\text{model } T\text{:} \qquad a(\mathbf{x},t) = f(u(\mathbf{x},t),\theta)\,, \tag{2.5}$$

to correlate $a$ with the state $u$ and model parameters $\theta \in \mathbb{R}^n$. Without loss of generality we can replace $a$ in (2.5) by $a_w$ because $a_{\mathrm{mol}}$ is assumed to be known.

**2.2. Incremental identification.** The incremental identification directly follows the steps of model development [20]. We assume throughout, that appropriate transient measurement data at sufficiently high resolution in space $\mathbf{x}$ and time $t$ are available.

We rewrite the balance equation (2.1) as

$$\frac{\partial u}{\partial t} + \mathbf{w}\cdot\nabla u = F \quad \text{in } \Omega \times (t_0,t_f]\,, \tag{2.6}$$

with

$$F(\mathbf{x},t) = -\nabla\cdot\mathbf{q}(\mathbf{x},t)\,, \quad (\mathbf{x},t) \in \Omega \times (t_0,t_f]\,. \tag{2.7}$$

Here we assumed for simplicity a constant density normalized to $\rho = 1$. In the first step of the incremental identification, the introduced (artificial) *source* $F(\mathbf{x},t)$ is estimated from the balance equation (2.6) with proper initial and boundary conditions, on the

basis of suitable measurement data $u_m(\mathbf{x},t)$. This is a typical example of a *source inverse problem* [2].

The incremental identification at the next level uses the estimated source $F(\mathbf{x},t)$ as model-based measurement data together with the transient measurements $u_m(\mathbf{x},t)$ to reconstruct the transport coefficient $a(\mathbf{x},t)$. Hence $a(\mathbf{x},t)$ is to be estimated from the equation

$$-\nabla\cdot(a\nabla u) = -F \quad \text{in } \Omega\times(t_0,t_f]\,, \tag{2.8}$$

which corresponds to a *coefficient inverse problem* [2].

In the third step of the identification procedure the function $a(\mathbf{x},t)$ should be correlated with states as in (2.5). Different model candidates involving the state $u$ and model parameters $\theta$ can be considered. The measurement data are to be used to estimate parameters for each candidate model. The best model is to be selected by carrying out a model discrimination between candidates using some measure of model validity.

In the remainder of this paper we address the inverse problems that arise in the first two steps of the incremental identification approach. The model discrimination issue in the third step is not considered here.

For the numerical treatment of the source inverse problem in the first step it is very convenient to consider a variant of (2.6) that uses the expression (2.4) for the transport coefficient. This leads to

$$F(\mathbf{x},t) = \nabla\cdot(a_{\mathrm{mol}}\nabla u(\mathbf{x},t)) + F_w(\mathbf{x},t)\,, \quad (\mathbf{x},t)\in\Omega\times[t_0,t_f]\,. \tag{2.9}$$

As a result, instead of $F(\mathbf{x},t)$ it suffices to estimate the enhanced part $F_w(\mathbf{x},t)$ of the source term on the basis of transient measurement data $u_m(\mathbf{x},t)$. Consequently, in the first step of the identification procedure one has to reconstruct the source term $F_w$ in the following *convection-diffusion* equation

$$\text{model } \overline{B}\text{:} \qquad \frac{\partial u}{\partial t} + \mathbf{w}\cdot\nabla u - \nabla\cdot(a_{\mathrm{mol}}\nabla u) = F_w \quad \text{in } \Omega\times(t_0,t_f]\,, \tag{2.10a}$$

with initial and boundary conditions

$$\begin{aligned} u(\mathbf{x},t_0) &= u_0(\mathbf{x})\,,\ \mathbf{x}\in\Omega\,,\\ u(\mathbf{x},t) &= g_D(\mathbf{x},t)\,,\ (\mathbf{x},t)\in\Gamma_D\times[t_0,t_f]\,,\\ \frac{\partial u}{\partial n}(\mathbf{x},t) &= g_N(\mathbf{x},t)\,,\ (\mathbf{x},t)\in\Gamma_N\times[t_0,t_f]\,. \end{aligned} \tag{2.10b}$$

Compared to (2.6) we now have a convection-diffusion problem instead of a pure convection problem. Due to the diffusion part the numerical treatment becomes easier. Furthermore, for $u$ we can now use the same boundary conditions as in (1.1b).

In the second step of the incremental identification one has to determine the coefficient in the diffusion equation

$$\text{model } \overline{F}\text{:} \qquad -\nabla\cdot(a_w^t\nabla u^t) = -F_w^t \quad \text{in } \Omega\,, \tag{2.11a}$$

with boundary conditions

$$\begin{aligned} u^t(\mathbf{x}) &= g_D^t(\mathbf{x})\,, \quad \mathbf{x}\in\Gamma_D\,,\\ \frac{\partial u^t}{\partial n}(\mathbf{x}) &= g_N^t(\mathbf{x})\,, \quad \mathbf{x}\in\Gamma_N\,. \end{aligned} \tag{2.11b}$$

Here, for a space and time dependent function $f(\mathbf{x},t)$ we introduce the notation $f^t(\mathbf{x}) := f(\mathbf{x},t)\,, (\mathbf{x},t) \in \Omega \times [t_0,t_f]$ to decouple the function values in time. In (2.11) we thus have a *stationary* diffusion problem for each given $t \in [t_0,t_f]$. Note that the transport coefficient $a(\mathbf{x},t)$ immediately follows from $a_w^t(\mathbf{x}) = a_w(\mathbf{x},t)$ due to (2.3).

We briefly compare the incremental identification approach to the simultaneous one. Recall the convection-diffusion equation (1.1a)

$$\text{model } \overline{BFT}\text{:} \qquad \frac{\partial u}{\partial t} + \mathbf{w}\cdot\nabla u - \nabla\cdot(a\nabla u) = 0 \quad \text{in } \Omega\times(t_0,t_f]\,. \tag{2.12a}$$

with initial and boundary conditions

$$\begin{aligned} u(\mathbf{x},t_0) &= u_0(\mathbf{x})\,, \quad \mathbf{x}\in\Omega\,,\\ u(\mathbf{x},t) &= g_D(\mathbf{x},t)\,, \quad (\mathbf{x},t)\in\Gamma_D\times[t_0,t_f]\,,\\ \frac{\partial u}{\partial n}(\mathbf{x},t) &= g_N(\mathbf{x},t)\,, \quad (\mathbf{x},t)\in\Gamma_N\times[t_0,t_f]\,. \end{aligned} \tag{2.12b}$$

While the incremental approach decomposes the identification process for the transport coefficient in steps, in the simultaneous one the model for the flux (2.2) and the relation (2.5) for the transport coefficient are collected in one equation (2.12a). Hence, all the assumptions made during the modeling will simultaneously influence the identification. Due to this, the level of uncertainty of the *simultaneous problem* (2.12) has increased, leading to a higher risk of poor estimates.

A further advantage of the incremental approach is that, for known velocity $\mathbf{w}(\mathbf{x},t)$ and molecular transport coefficient $a_{\mathrm{mol}}$, it suffices to reconstruct the source $F_w(\mathbf{x},t)$ at the first level and the enhanced transport coefficient $a_w(\mathbf{x},t)$ at the second level only *once*. The complexity due to the elimination of candidate models for the transport coefficient affects the third (final) level *only*, thus allowing for a more systematic derivation of suitable candidate models.

Compared to the simultaneous problem (2.12) where a nonlinear coefficient inverse problem in space and time has to be solved, the incremental identification procedure has advantages from the optimization point of view. The reconstruction of the source in the first step results in a *dynamical* optimization problem, which is *affine-linear*. The latter property implies that relatively (compared to a strongly nonlinear case) simple and efficient optimization methods can be applied. In the second step of the identification we have to deal with a nonlinear coefficient inverse problem which, however, is of steady-state type for each given time $t$, cf. (2.11). In this sense the incremental approach decouples dynamics and nonlinearity, which has advantages for the numerical treatment of these inverse problems.

The estimation problems arising in the incremental approach are typical inverse problems, ill-posed by their nature. This makes however, the question of error propagation through the sequence of inverse problems crucial for the approach. This issue is studied for the illustrative model problem in Section 4.

**3. Formulation and solution of the inverse problems.** The inverse problems resulting in the first two incremental steps are formulated as optimization problems [2]. In the first step of the incremental identification, the source $F_w$ should minimize the quadratic objective functional

$$J_1(F_w) = \frac{1}{2}\int_{t_0}^{t_f}\int_\Omega [u(\mathbf{x},t;F_w) - u_m(\mathbf{x},t)]^2 d\mathbf{x}\,dt\,, \tag{3.1}$$

with suitable transient measurement data $u_m(\mathbf{x},t)\,,(\mathbf{x},t)\in\Omega\times[t_0,t_f]$. Here $u(\mathbf{x},t;F_w)$ is the solution of the *direct problem* (2.10) with known initial condition $u_0$, and boundary conditions $g_D$ and $g_N$. We refer to the solution of the direct problem (2.10) as $u(\mathbf{x},t;F_w)$ to emphasize the dependence of the function $u$ on the unknown source $F_w$.

Similarly, the second identification step concerns the estimation of the enhanced transport coefficient $a_w$, using the previously estimated source $F_w$ and the transient measurement data $u_m(\mathbf{x},t)$. The optimization based formulation of this coefficient inverse problem consists of the minimization of the objective functional

$$J_2(a_w^t)=\frac{1}{2}\int_\Omega[u^t(\mathbf{x};a_w^t)-u_m^t(\mathbf{x})]^2d\mathbf{x}\,. \tag{3.2}$$

Here $u^t(\mathbf{x};a_w^t)$ denotes the solution of the direct problem (2.11) for given $a_w$.

**3.1. Numerical solution strategy.** For the solution of the optimization problems the conjugate gradient (CG) method is used [12, 21]. In this paper, regularization is only introduced via spatial and temporal discretization and by means of a suitable stopping criterion for the CG algorithm. Hence, for a given discretization the number of CG iterations serves as a regularization parameter [11]. Either the heuristic L-curve method [17] or the discrepancy principle [11] is used to determine an appropriate value of this parameter.

To be able to explain the role of the sensitivity and adjoint problems in this context, we describe the general structure of the CG method. Let $H$ be a given (Hilbert) space with scalar product denoted by $(\cdot,\cdot)_H$. We introduce a functional $J:H\to\mathbb{R}$, for which a (local) minimum should be determined, defined by

$$J(f)=\big(u(f)-u_m,\ u(f)-u_m\big)_H.$$

Here $f$ denotes the function to be estimated, $u(f)$ the solution of a given corresponding direct problem and $u_m$ the measurement data. The CG method consists of the following steps:

(i) Set $n\leftarrow 0$ and choose an initial guess $f^0\in H$ .

(ii) If the objective function satisfies a given tolerance criterion then stop, otherwise continue .

(iii) Calculate the new search direction as

$$p^n=-\nabla J(f^n)+\gamma^n p^{n-1}\,, \tag{3.3}$$

with

$$\gamma^n=\frac{\big(\nabla J(f^n),\nabla J(f^n)\big)_H}{\big(\nabla J(f^{n-1}),\nabla J(f^{n-1})\big)_H},\quad \text{for}\ \ n\geq 1\quad\text{and}\quad \gamma^0:=0. \tag{3.4}$$

(iv) Calculate a *step length* by solving (approximately) the one-dimensional minimization problem

$$\mu^n=argmin_{\mu\geq 0}J(f^n+\mu p^n)\,. \tag{3.5}$$

In case of an affine-linear problem the optimal step length is given by

$$\mu^n=\frac{\big(u(f^n)-u_m,S(f^n,p^n)\big)_H}{\big(S(f^n,p^n),S(f^n,p^n)\big)_H}\,, \tag{3.6}$$

with $S$ the solution of the *sensitivity problem* (cf. Subsections 3.1.1, 3.1.2).

(v) Update the approximation according to

$$f^{n+1} = f^n + \mu^n p^n \,. \tag{3.7}$$

(vi) Set $n \leftarrow n+1$ and repeat the procedure down from (ii).

In the CG method one has to calculate the gradient of the objective functional $\nabla J(f^n)$. This gradient can be determined from the solution of an *adjoint problem*. The calculation of a step length in (iv) requires the solution of the sensitivity problem (cf. below). In the nonlinear case, the formula (3.6) is pragmatically used as an *approximate* solution of the problem (3.5). We do not give a derivation of the adjoint and the sensitivity problems, since this can be found in the literature, e.g. [1, 2]. The resulting adjoint and sensitivity problems corresponding to the optimization problems in the first two steps of the incremental identification procedure are given in the subsections below.

**3.1.1. Estimation of the source $F_w(\mathbf{x}, t)$.** The sensitivity problem corresponding to (2.10) is given by

$$\frac{\partial S_1}{\partial t} + \mathbf{w} \cdot \nabla S_1 - a_{\mathrm{mol}} \Delta S_1 = \tilde{F_w} \quad \text{in } \Omega \times (t_0, t_f] \,, \tag{3.8a}$$

$$\begin{aligned} S_1(\mathbf{x}, t_0) &= 0 \,, \quad \mathbf{x} \in \Omega \,, \\ S_1(\mathbf{x}, t) &= 0 \,, \quad (\mathbf{x}, t) \in \Gamma_D \times [t_0, t_f] \,, \\ \frac{\partial S_1}{\partial n}(\mathbf{x}, t) &= 0 \,, \quad (\mathbf{x}, t) \in \Gamma_N \times [t_0, t_f] \,. \end{aligned} \tag{3.8b}$$

where $\tilde{F_w}(\mathbf{x}, t)$ is a perturbation of the unknown source $F_w$. This partial differential equation has exactly the same structure as the corresponding direct problem (2.10), only the initial and boundary conditions are different. The step length is determined from (3.6) (which results in the optimal one, due to the affine-linearity) where $S$ is replaced by $S_1 = S_1(\mathbf{x}, t; F_w, \tilde{F_w})$, the solution of the sensitivity problem (3.8) with $\tilde{F_w} = p^n$.

It can be shown that the gradient of the objective functional satisfies

$$\nabla J_1(F_w) = \varphi_1 \quad \text{in } \Omega \times [t_0, t_f] \,, \tag{3.9}$$

where the adjoint variable $\varphi_1$ is the solution of the following adjoint problem:

$$-\frac{\partial \varphi_1}{\partial t} - \mathbf{w} \cdot \nabla \varphi_1 - a_{\mathrm{mol}} \Delta \varphi_1 = [u(F_w) - u_m] \quad \text{in } \Omega \times [t_0, t_f) \,, \tag{3.10a}$$

$$\begin{aligned} \varphi_1(\mathbf{x}, t_f) &= 0 \,, \quad \mathbf{x} \in \Omega \,, \\ \varphi_1(\mathbf{x}, t) &= 0 \,, \quad (\mathbf{x}, t) \in \Gamma_D \times [t_0, t_f] \,, \\ \frac{\partial \varphi_1}{\partial n}(\mathbf{x}, t) &= 0 \,, \quad (\mathbf{x}, t) \in \Gamma_N \times [t_0, t_f] \,. \end{aligned} \tag{3.10b}$$

Opposite to the direct problem (2.10), we now have a condition at the final time $t_f$. Going backwards in time (by introducing a new time variable $t_f - t$) this equation shows exactly the same structure as the direct problem, only with different initial and boundary conditions. We do not give the derivation of the identity (3.9) since it follows from a standard procedure, cf. [2]. The adjoint variable immediately yields the required gradient of the objective functional in the CG method.

Thus, the CG algorithm for minimizing $J_1$ requires per iteration the solution of three very similar problems, namely the direct, the adjoint and the sensitivity

problem. However, due to the linearity of the involved equations only *two* problems - the sensitivity (3.8) and the adjoint (3.10) problem - have to be solved. Instead of solving the direct problem (2.10) for $u(\mathbf{x}, t; F_w)$, the linear update formula

$$u(F_w^{n+1}) = u(F_w^n) + \mu^n S_1(F_w^n, \tilde{F}_w^n) \tag{3.11}$$

can be applied.

In [14] we considered a similar inverse problem, where a boundary heat flux in a nonstationary three-dimensional heat conduction problem is estimated from boundary temperature measurements in a falling film experiment. The solution approach presented therein has the same structure as for the source estimation described above.

**3.1.2. Estimation of the coefficient $a_w(\mathbf{x}, t)$.** The approach used for minimizing $J_2$ is very similar to the one used in the previous subsection. However, the nonlinearity of the problem leads to some differences. Per iteration the CG method requires the solution of a direct, an adjoint and a sensitivity problem. Due to the nonlinearity of the estimation problem, the direct problem (2.11) has to be solved in each iteration since a simple update formula as in (3.11) is not valid.

The sensitivity problem for (2.11) is given by

$$-\nabla \cdot (a_w^t \nabla S_2^t) = \nabla \cdot (\tilde{a}_w^t \nabla u^t) \quad \text{in } \Omega\,, \tag{3.12a}$$

$$\begin{aligned} S_2^t(\mathbf{x}) &= 0\,, \quad \mathbf{x} \in \Gamma_D\,, \\ \frac{\partial S_2^t}{\partial n}(\mathbf{x}) &= 0\,, \quad \mathbf{x} \in \Gamma_N\,, \end{aligned} \tag{3.12b}$$

where for each time $t \in [t_0, t_f]$, $S_2^t = S_2^t(\mathbf{x}; a_w^t, \tilde{a}_w^t)$ is the first order perturbation of the function $u^t(\mathbf{x}; a_w^t)$ caused by a perturbation $\tilde{a}_w^t(\mathbf{x})$ of the enhanced transport coefficient $a_w^t(\mathbf{x})$. Here, $u^t = u^t(\mathbf{x}; a_w^t)$ in the right-hand side in (3.12a) denotes the solution of the corresponding direct problem (2.11) for the given value of $a_w^t(\mathbf{x})$. This equation has the same structure as the corresponding direct problem. Note, however, that apart from the different boundary conditions one also has a specific right-hand side in this sensitivity equation. This distinctive term arises due to the nonlinearity of the coefficient inverse problem. The step length is obtained from (3.6) if for given time $t$, $\tilde{a}_w^t$ is replaced by $p^n$ in the sensitivity equation (3.12).

A standard derivation [2] yields the following expression for the gradient

$$\nabla J_2(a_w^t) = \nabla \varphi_2^t \cdot \nabla u^t(a_w^t) \quad \text{in } \Omega\,, \tag{3.13}$$

for each given $t \in [t_0, t_f]$. The adjoint variable $\varphi_2^t$ at time $t$ is the solution of the following adjoint problem

$$-\nabla \cdot (a_w^t \nabla \varphi_2^t) = [u^t(\mathbf{x}; a_w^t) - u_m^t(\mathbf{x})] \quad \text{in } \Omega\,, \tag{3.14a}$$

$$\begin{aligned} \varphi_2^t(\mathbf{x}) &= 0\,, \quad \mathbf{x} \in \Gamma_D\,, \\ \frac{\partial \varphi_2^t}{\partial n}(\mathbf{x}) &= 0\,, \quad \mathbf{x} \in \Gamma_N\,, \end{aligned} \tag{3.14b}$$

which has the same structure as the direct problem (2.11), due to the symmetry of the diffusion operator $\nabla \cdot (a_w^t \nabla(\,\cdot\,))$.

From (3.13) one obtains the gradients needed in the CG algorithm.

**3.1.3. Solution of the direct problems.** The direct, sensitivity and adjoint problems used in the CG method have the same structure. Since all these problems are of elliptic type, similar numerical techniques can be employed for their solution. In case of source estimation, the three convection-diffusion problems are solved with exactly the same code. For the coefficient estimation all the three corresponding steady-state diffusion problems are solved with the same software code as well.

The solutions of the 3D problems arising during the estimation of the unknown source and transport coefficient are calculated by means of the software package DROPS [10]. DROPS is based on multi-level nested grids and conforming finite element discretization methods. For time discretization a standard one-step $\theta$-method is used. For the space discretization piecewise linear finite elements on a tetrahedral grid are employed. The resulting discrete systems of linear equations are solved by suitable iterative Krylov subspace methods. In case of the convection-diffusion equations (2.10), (3.8), (3.10) we use a preconditioned Generalized Minimal Residuals (GMRES) method, and for the diffusion problems (2.11), (3.12), (3.14) a preconditioned conjugate gradient (PCG) method is applied [25]. For the simulations presented in this paper the SSOR method is used for preconditioning. Other options, for example multigrid solvers, are available in DROPS. In this paper we do not study efficiency of these solvers for the direct, the sensitivity and the adjoint problems. We use a fixed (quasi-uniform) mesh for discretization and prescribe a tolerance with which the discrete linear systems are solved.

**4. Illustrative case study.** In this section the incremental approach is illustrated for a problem that is motivated by research on the identification of energy transport in laminar wavy film flows. The complex dynamics of the nonlinear surface waves typically present in film flows [13, 22] renders a direct transient simulation in 3D numerically very complicated and computationally expensive. Therefore, manageable *approximate* descriptions, yet accurately modeling the underlying transport processes, have gained increasing importance in the engineering literature to support the design of technical systems [6]. A possible simplified model is as follows. In order to reduce the problem complexity, the 3D time-varying domain $\Omega_W$ corresponding to the liquid phase is mapped to a 3D time-invariant waveless domain $\Omega := (0, L_x) \times (0, L_y) \times (0, L_z) \subset \mathbb{R}^3$. This reduction is compensated by the introduction of a space and time dependent *effective* transport coefficient $a_{\text{eff}}(\mathbf{x}, t)$ [6, 9, 28], to capture all wave-induced transport effects in this flat film geometry. Such a flat film model is considered in the remainder. It consists of a convection-diffusion system that describes an energy transport in a single component fluid on the flat (rectangular) domain $\Omega$ with boundary $\Gamma = \partial\Omega$, and its parts $\Gamma = \Gamma_{in} \cup \Gamma_{wall} \cup \Gamma_{out} \cup \Gamma_r$ defined as

$$
\begin{aligned}
\Gamma_{in} &= \{(x, y, z) \in \Gamma : \ x = 0\} \subset \Gamma_D - \text{ the inflow boundary}, \\
\Gamma_{wall} &= \{(x, y, z) \in \Gamma : \ y = 0\} \subset \Gamma_D - \text{ the wall boundary}, \\
\Gamma_{out} &= \{(x, y, z) \in \Gamma : \ x = L_x\} \subset \Gamma_N - \text{ the outflow boundary}, \\
\Gamma_r &= \Gamma \setminus (\Gamma_{in} \cup \Gamma_{wall} \cup \Gamma_{out}) \subset \Gamma_N - \text{ the remaining boundaries}.
\end{aligned}
$$

In this case study, the state variable $u(\mathbf{x}, t)$ in (1.1) is the temperature $T(\mathbf{x}, t)$ and the transport coefficient $a(\mathbf{x}, t)$ the *effective thermal diffusivity*. The unit cube $\Omega = (0, 1)^3 [mm^3]$ is considered as computational domain for simplicity of presentation and to avoid possible numerical complications due to anisotropy effects. $x$ corresponds to the flow direction of the falling film and $y$ is the direction along the film thickness. The velocity $\mathbf{w}(\mathbf{x}, t)$ is given by a Nusselt-profile, i.e. $\mathbf{w}(\mathbf{x}, t) = 4.2857(2y - y^2)$ [23].

The effective thermal diffusivity to be estimated in the first two steps of the incremental identification approach is chosen to be time-independent and is denoted by $a_{\text{eff}}^{ex}(\mathbf{x}), \mathbf{x} \in \Omega$. With an intuitive notion of the physical quantity, $a_{\text{eff}}^{ex}$ is chosen to have a sinusoidal pattern in the flow direction $x$ of the falling film and a linear profile along the other two directions, with a larger gradient in the $y$-direction (film thickness) than in the $z$-direction:

$$a_{\text{eff}}^{ex}(\mathbf{x}) = 0.35 + 7(1.1 + \sin(3x) + \frac{y}{5} + \frac{z}{50}), \quad (x, y, z) \in \Omega. \tag{4.1}$$

The material properties of the fluid are lumped in the constant *molecular thermal diffusivity* $a_{\text{mol}}^{ex} = 0.35\frac{mm^2}{s}$, whereas the remaining part of the effective thermal diffusivity $a_{\text{eff}}^{ex}(\mathbf{x})$ represents the *wavy thermal diffusivity* $a_w^{ex}(\mathbf{x})$, the transport coefficient capturing the wave-induced effects in the flat film model.

In the first step of the incremental identification, we use the implicit Euler scheme with time step $\tau = 0.01s$ and apply 50 time steps. The initial condition is a constant, i. e. $T(\mathbf{x}, t_0) = 7°C, \mathbf{x} \in \Omega$. The known Dirichlet boundary conditions are chosen to have linear profiles. The inflow temperature drops from $17°C$ to $10°C$ along the $y$ axis, i. e. $T_{in}(\mathbf{x}, t) = -7y + 17$, whereas the wall temperature rises from $17°C$ to $27°C$ along the $x$ axis, i. e. $T_{wall}(\mathbf{x}, t) = 10x + 17$. At the Neumann boundaries $\Gamma_{out}$ and $\Gamma_r$ the natural condition is used, i. e. they are assumed to be perfectly isolated. For the initial approximation in the optimization procedure, due to the lack of better information, we choose $F_w^0(\mathbf{x}, t) = 0, (\mathbf{x}, t) \in \Omega \times [t_0, t_f]$.

In the second step of the identification, the same boundary conditions are used. The time interval $[t_0, t_f]$ is decoupled in 50 time steps and the estimation of the wavy thermal diffusivity is carried out separately for each time interval. Note that per time interval we then have to solve a stationary inverse diffusion coefficient problem. The initial time $t_0$ is a singular point, because the initial temperature is constant and no reconstruction is possible since the coefficient is not uniquely defined in this case (cf. (2.10)).

As expected, the choice of a suitable initial vector for the optimization method is much more important for the *non*linear optimization problem in the second identification step than for the linear one in the first step. We do not address this issue of initialization of the optimizer here. In all our experiments we use

$$a_w^{initial}(\mathbf{x}) = 7(1.1 + x\sin(3) + \frac{y}{5} + \frac{z}{50}), \quad (x, y, z) \in \Omega, \tag{4.2}$$

as initial guess for the wavy thermal diffusivity in the first time step, cf. Figure 4.1. With this choice we always observed convergence of the CG method towards the desired minimum of the nonlinear functional.

In the spatial discretization we use a uniform mesh consisting of $24 \times 24 \times 19$ intervals in $x, y$ and $z$ directions, respectively, which yields a space discretization with 11520 unknowns and 65664 tetrahedra.

The estimation results with error-free measurements will be considered first. As measurement data, we take the temperature $T_m$ obtained from the solution of the simultaneous problem (2.12) with the chosen quantity $a_{\text{eff}}^{ex}$ (cf. (4.1)) as the corresponding effective thermal diffusivity.

**4.1. Estimation with error-free measurements.** In Fig. 4.2 (a) the objective functional $J_1(F_w)$ is plotted over the number of optimization iterations. In Fig. 4.2 (b) the source $F_w(\mathbf{x}, t)$ is plotted as a function of $x$ for fixed $y = 0.5\,mm$ and

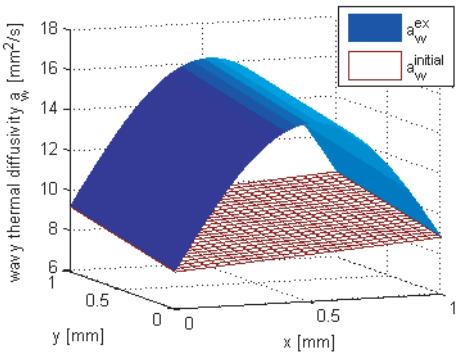


FIG. 4.1. *Initial approximation for the wavy thermal diffusivity* $a_w^t$ *at constant* $z = 0.5\,mm$.

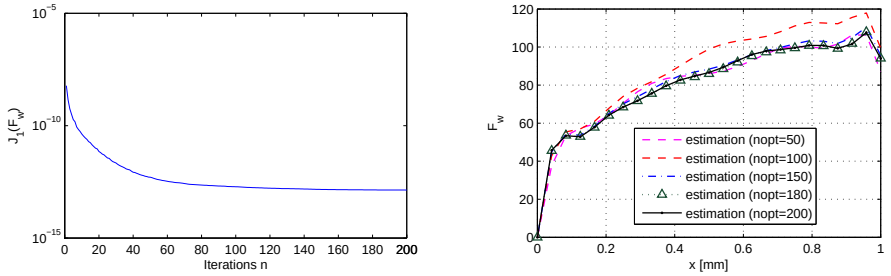


(a) (b)

FIG. 4.2. *(a) Objective functional* $J_1$. *(b) Estimated source* $F_w$ *for different iterations nopt at time* $t = 0.04s$, $y = 0.5\,mm$ *and* $z = 0.5\,mm$.

$z = 0.5\,mm$ (i. e. at the middle of the $y-$ and $z-$ coordinates, respectively) at a certain time for different iterations of the optimization, denoted by *nopt*. Snapshots of the estimated source $F_w^{200}(\mathbf{x}, t)$ at the end of the optimization procedure ($nopt = 200$) are presented in Fig. 4.3.

Note that during the optimization the initial approximation at the boundaries $\Gamma_{in}$ (the plane $x = 0\,mm$) and $\Gamma_{wall}$ (the plane $y = 0\,mm$) could not be improved, since the gradient of the objective functional $J_1(F_w)$ is always zero along these boundaries. This follows directly from the boundary conditions of the corresponding adjoint problem (3.10) and the expression (3.9) for the gradient $\nabla J_1(F_w)$.

The estimation of the wavy thermal diffusivity in the second step of our incremental approach uses the estimated source $F_w^{200}(\mathbf{x}, t)$ at iteration $nopt = 200$ and the temperature $T_m(\mathbf{x}, t)$ (for fixed $t$). Although the exact value $a_w^{ex}$ is time-independent in this case study, the estimated value is time-dependent. We use a superscript $t$ in the notation, i.e. $a_w^{ext}(\mathbf{x})$, to indicate explicitly the estimation from the source $F_w^t(\mathbf{x})$ and the temperature $T_m^t(\mathbf{x})$ at given time $t$. We choose (4.2) as an initial approximation for the time $t = 0.01s$, whereas the estimation computed for $t = 0.01s$ is used for later times $t > 0.01s$.

The estimates of the wavy thermal diffusivity for $z = 0.5\,mm$ at selected times are shown in Fig. 4.4 (a), whereas Fig. 4.4 (b) shows contour lines of the difference between the exact and estimated quantities. The estimates in these figures have been obtained using 250 CG iterations for time $t = 0.01s$ and 200 CG iterations for

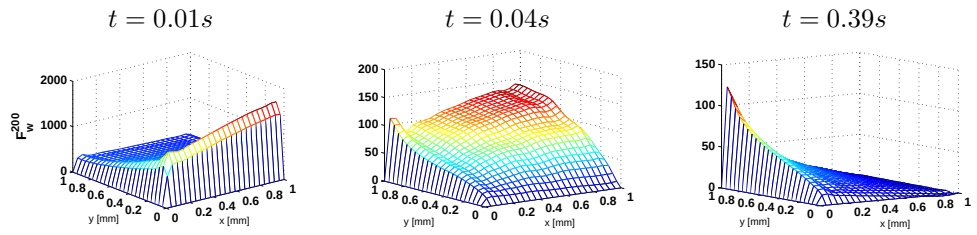


FIG. 4.3. *Estimated source $F_w$ at different times for constant $z = 0.5\,mm$ with unperturbed measurements for nopt = 200.*

later times. We see from these plots, that the estimation quality for times $t > 0.01s$ improves considerably over the estimation obtained at $t = 0.01s$. One reason for this is the better initial approximation for later times.

A closer look at the results reveals also that at a fixed time the estimates in the $y$-direction (i.e. film thickness) is better for small values of $y$ than for larger ones. Moreover, the region of good estimation results gets larger with increasing time. These effects are illustrated in Fig. 4.5 where the estimates $a_w^t(\mathbf{x})$, $t \in \{0.01s, 0.04s, 0.39s\}$ are presented as a function of $x$ for $y \in \{0\,mm, 0.5\,mm, 1\,mm\}$ and $z = 0.5\,mm$. Estimates for different optimization iterations *nopt* are also shown in the figures. This behaviour is expected because of the dynamics of the system. At small times, the boundary conditions at $\Gamma_{wall} = \{y = 0\,mm\}$ influence only a small region near the wall, such that not enough information is available for a good reconstruction of the wavy thermal diffusivity $a_w^t$ for larger values of $y$. Therefore, good estimates are obtained at $\Gamma_{wall}$ for all times. As time increases, the estimation quality gets better also in regions away from the wall. This is illustrated in Fig. 4.6, which shows estimates of the wavy thermal diffusivity at $y = 1\,mm$ and $z = 0.5\,mm$ for different times.

**4.2. Estimation in the presence of measurement errors.** In this section, we perturb the temperature $T_m$ by an artificial measurement error $\omega$. The values of $\omega$ are generated from a zero mean normal distribution with variance one. We compute the perturbed temperature $\tilde{T}_m$ by

$$\tilde{T}_m = T_m + \sigma\omega\,,$$

with $\sigma$ being the standard deviation of the measurement error. The parameter $\sigma$ is used to control the amount of error added to the exact data. We take the values $\sigma_1 = 0.07$ and $\sigma_2 = 0.125$ in the following simulation experiments.

In the presence of measurement errors, an increasing number of iterations eventually leads to a poorer estimation quality due to the undesirable effect that measurement errors are resolved. Therefore, a compromise between the residual and the solution norm has to be established by an appropriate regularization [17]. Besides the regularizing effect of discretization, the number of CG iterations is used as a regularization parameter. An appropriate value for this parameter can be obtained by the L-curve, which is a parameterized plot of the residual against a solution norm.

The results for the source term estimation will be presented first. The L-curve plot is shown in Fig. 4.7. This curve suggests that $nopt = 97$ and $nopt = 59$ are reasonable regularization parameters for $\sigma_1$ and $\sigma_2$, respectively. The snapshots of the regularized solutions for the values of $\sigma_1\,, \sigma_2$, the optimal estimates $F_w^{nopt}(\mathbf{x}, t)$

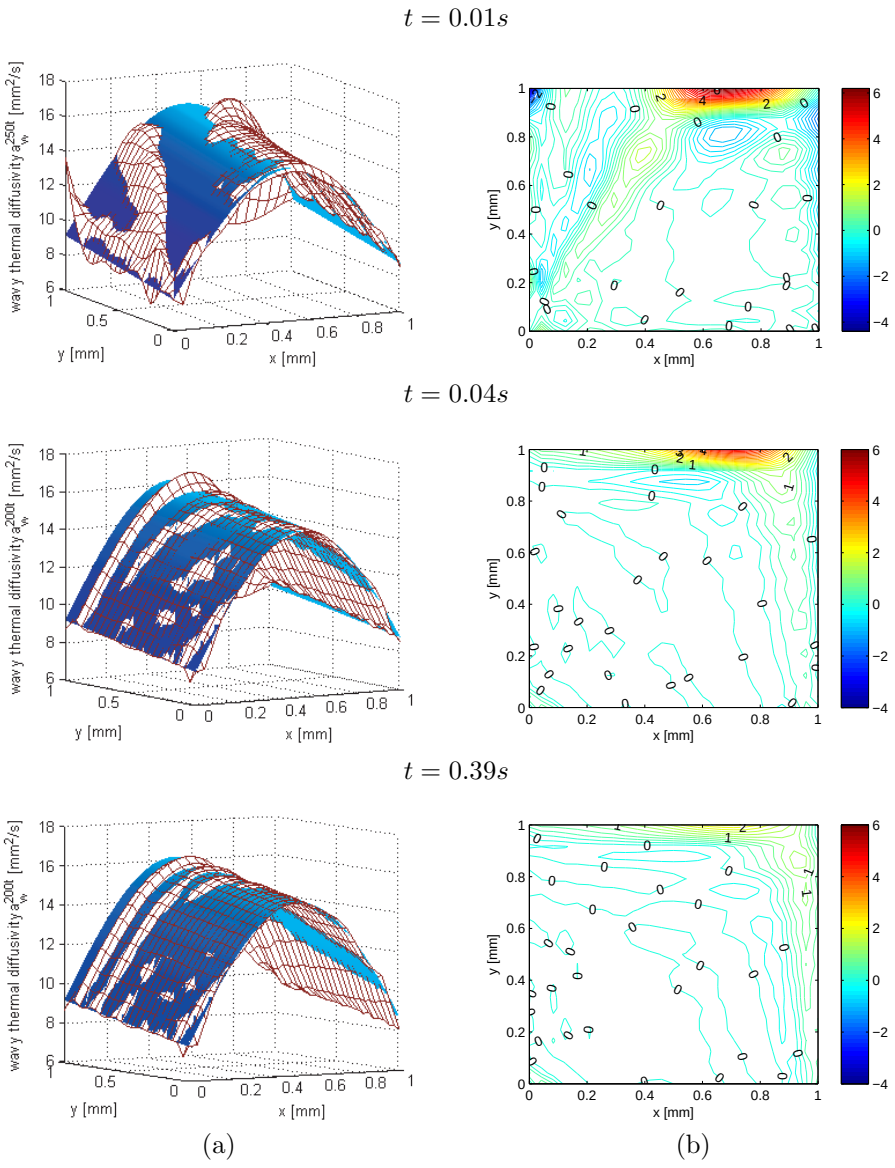


FIG. 4.4. *(a) Estimated (meshed surface) and exact (shaded surface) wavy thermal diffusivities $a_w^t$, (b) deviation between exact and estimated wavy thermal diffusivities $a_w^t$ at different times.*

are shown in Fig. 4.8 and Fig. 4.9, respectively, for constant $z = 0.5\,mm$. Due to the errors in the measurements, the estimates are no longer smooth, but the qualitative behaviour is the same (cf. Fig. 4.3).

The estimation $F_w^{nopt}(\mathbf{x}, t)$ obtained with perturbed data for $\sigma_1$ and $\sigma_2$ is compared to the estimates $F_w^{200}(\mathbf{x}, t)$ obtained with exact data in the previous section. The results are shown in Fig. 4.10 as a function of $x$ for fixed $y = 0.5\,mm\,, z = 0.5\,mm$ and three different $t$-values. The corresponding temperatures are presented for the case of $\sigma_1$ in Fig. 4.11. For $\sigma_2$, similar results are obtained.

The regularization parameter can be determined alternatively using the discrep-

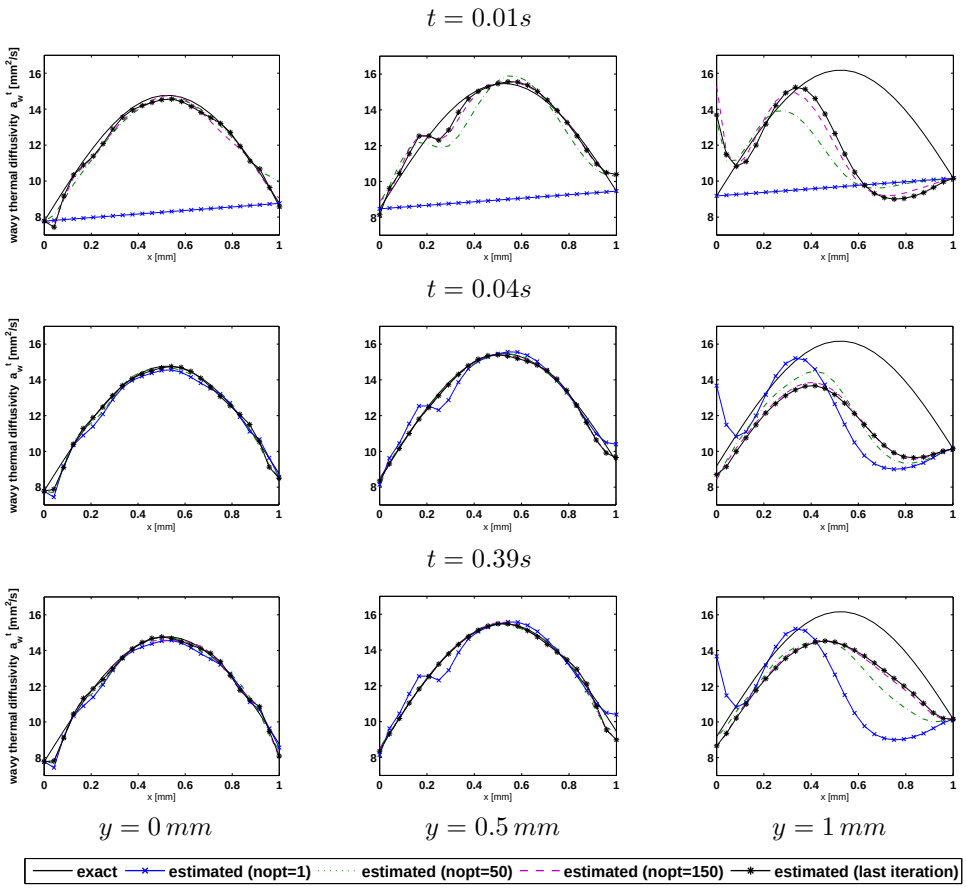


FIG. 4.5. *Estimated wavy thermal diffusivity $a_w^t$ at different optimization iterations nopt for different times, different $y$ and $z = 0.5\,mm$.*

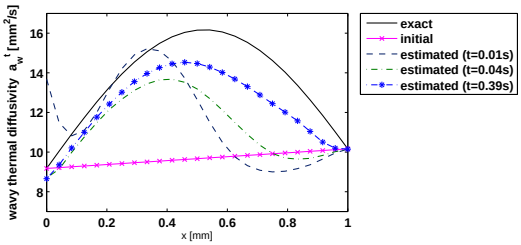


FIG. 4.6. *Estimates of wavy thermal diffusivity $a_w^t$ for constant $y = 1\,mm$ and $z = 0.5\,mm$ at different times.*

ancy principle [11]. Here the knowledge of the error's magnitude is used to propose the stopping condition for the objective functional, in the sense that the iterations are stopped when the residual approximately equals the error level $\sigma$. Using (3.1), we

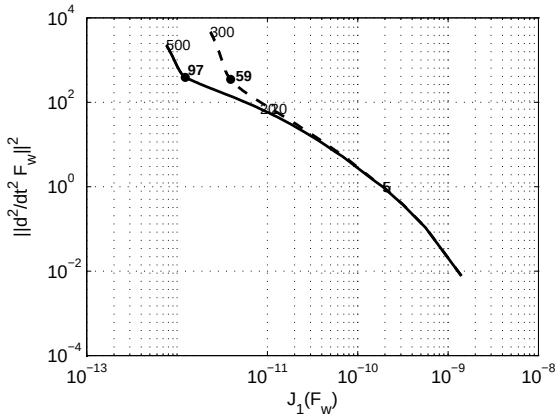


FIG. 4.7. *L-curve for source estimation based on perturbed measurements with* $\sigma_1 = 0.07$ *(solid curve) and* $\sigma_2 = 0.125$ *(dashed curve).*

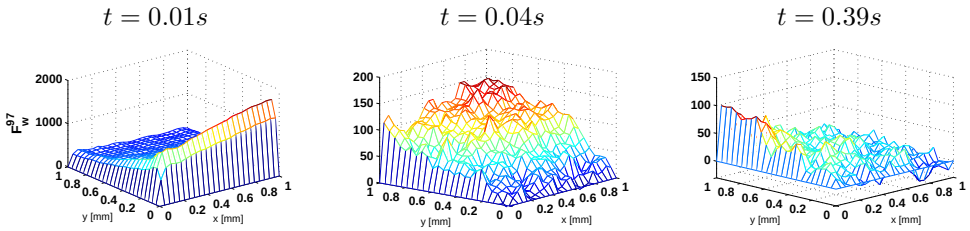


FIG. 4.8. *Estimated source* $F_w$ *at different times for constant* $z = 0.5\,mm$ *with perturbed measurements* ($\sigma_1 = 0.07$) *for* $nopt = 97$.

get the following condition for the objective $J_1(F_w^n)$

$$J_1(F_w^n) < \kappa_1(t_f - t_0)V\sigma\,, \tag{4.3}$$

where $V$ is the volume of $\Omega$, and $\kappa_1 > 1$. For a value of $\kappa_1 = 1.01$, the optimal number of iterations is $nopt = 97$ in case of $\sigma_1$ and $nopt = 59$ in case of $\sigma_2$, hence, (accidentally) the same values as those obtained by the L-curve.

For the estimation of the wavy thermal diffusivity, the regularized optimal solutions $F_w^{nopt}(\mathbf{x}, t)$ and the measurement data $\tilde{T}_m$ are used in the corresponding direct problem (2.11). We apply the L-curve and the discrepancy principle in order to find the optimal value for the number of CG iterations. In the discrepancy principle, the stopping condition for the objective functional $J_2(a_w^{n\,t})$ is written similarly to (4.3) as

$$J_2(a_w^{n\,t}) < \kappa_2 V\sigma\,. \tag{4.4}$$

At time $t = 0.01s$, the L-curve principle suggests an optimal value of $nopt = 16$ in case of $\sigma_1$ and $nopt = 10$ for $\sigma_2$. With $\kappa_2 = 1.001$, the discrepancy principle resulted in $nopt = 12$ and $nopt = 8$ for $\sigma_1$ and $\sigma_2$, respectively. At times $t \in \{0.04s, 0.39s\}$, the L-curve principle predicted $nopt = 18$ for $\sigma_1$ and $nopt = 9$ for $\sigma_2$, whereas for the chosen value of $\kappa_2$, the discrepancy principle at these times yielded $nopt = 7$ and $nopt = 5$ iterations for $\sigma_1$ and $\sigma_2$, respectively. For other choices of $\kappa_2$ we would have obtained other values for $nopt$ by the discrepancy principle. After trying a few

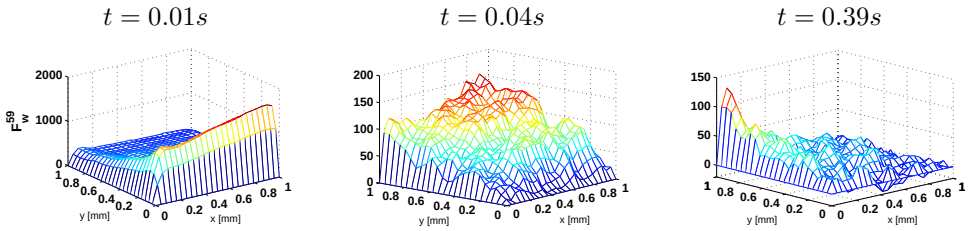


FIG. 4.9. *Estimated source $F_w$ at different times for constant $z = 0.5\,mm$ with perturbed measurements ($\sigma_2 = 0.125$) for nopt $= 59$.*

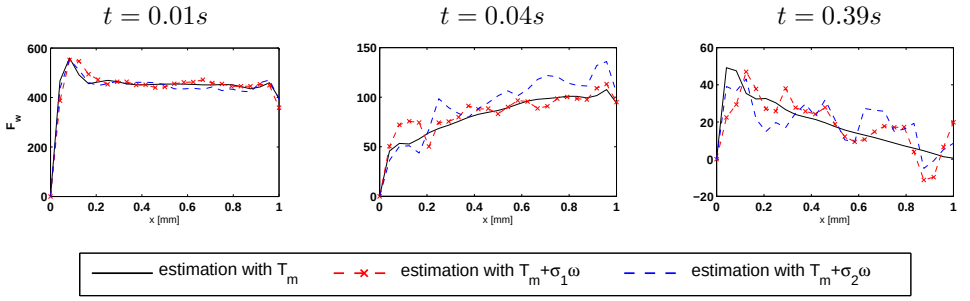


FIG. 4.10. *Estimated source $F_w$ with unperturbed measurements for nopt $= 200$ and perturbed measurements for nopt $= 97$ ($\sigma_1 = 0.07$) and for nopt $= 59$ ($\sigma_2 = 0.125$) at different times.*

other values for the parameter $\kappa_2$ we decided for $\kappa_2 = 1.001$ as this choice yielded reasonable results. The corresponding L-curves are shown in Fig. 4.12. For $t > 0.01s$ the L-curve has a nonmonotonic form.

In experiments we see that the estimates obtained by the discrepancy principle for the noise level $\sigma_2$ are smoother but still over-regularized, whereas those suggested by the L-curve method contain oscillations but are closer to the exact quantity. For $\sigma_1$, the estimates obtained by the discrepancy principle compared to the L-curve are smoother as well as closer to the exact quantity. A good understanding of the regularizing effect of the CG method for this type of problems is still lacking [17]. Hence, the choice of an appropriate value for the regularization parameter is rather problem-dependent and relies to a large extent on user experience. In Fig. 4.13, the optimal regularized estimates for the two noise levels obtained by the discrepancy principle are presented as a function of $x$ for $z = 0.5\,mm$ and different values of $y$. Due to the reasons stated above in the noise free case, we see again, for small times, that estimates near the wall $y = 0\,mm$ are better than estimates at larger $y$. The estimates for $t = 0.01$ have been used as initial approximations for $t > 0.01s$.

Compared to the error-free case, these results show similar trends. The estimates obtained at the beginning time $t = 0.01s$ are of an acceptable quality only at $y = 0\,mm$, i. e. near the wall, where the estimation quality was also the best in case of unperturbed measurements (cf. Fig. 4.5). The estimation quality for times $t > 0.01s$ improves considerably over those obtained at $t = 0.01s$. At each fixed time, the estimates in the $y$-direction (i.e., film thickness) are better for small values of $y$ than for larger ones, but as time increases, the region of acceptable reconstruction gets larger.

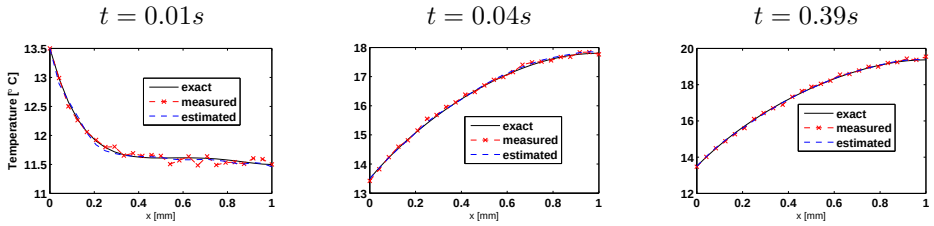


FIG. 4.11. *Exact, measured and estimated temperature for* $\sigma_1 = 0.07$ *at different times.*

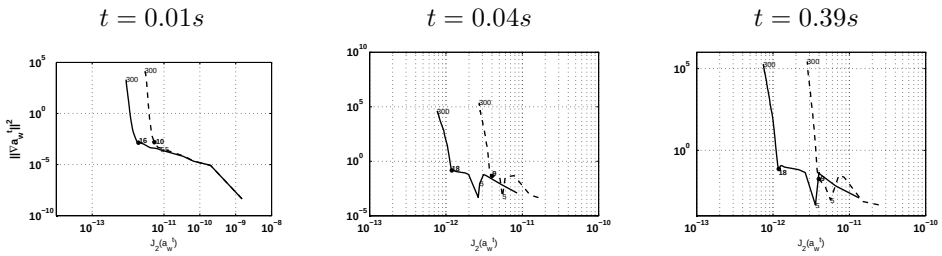


FIG. 4.12. *L-curves for coefficient estimation based on perturbed measurements with* $\sigma_1 = 0.07$ *(solid curve) and* $\sigma_2 = 0.125$ *(dashed curve) at different times.*

**5. Conclusions and outlook.** The method of incremental modeling and identification of transport phenomena in convection-diffusion systems is presented. The application of the incremental method to this class of problems is new. The simultaneous model is split into three hierarchically structured submodels. The identification problems in the first two steps (levels) have to be solved only once. The discrimination between several candidate models for the transport coefficient can be done in the third step.

The approach is illustrated on the identification of an effective thermal diffusivity in a three dimensional convection-diffusion problem that is similar to a flat film model used to investigate energy transport in laminar wavy film flows. The first step of the incremental identification is rather easy to handle due to the linearity of the corresponding source inverse problem. The results obtained at this level are quite satisfactory both for error-free and noisy measurements. The second step of the identification is far more complex due to the strong nonlinearity and extreme ill-posedness of the coefficient inverse problem that has to be solved. For satisfactory results one needs an initial approximation in the CG method which is sufficiently close to the solution. The interplay between the the two steps both with and without measurement errors is investigated.

In this paper we do not study the third (final) step in the incremental approach, in which a constitutive relation for the transport coefficient has to be determined. For each candidate model the best one is chosen by discriminating between the candidates using some reasonable model fit [27]. Besides to this third identification step our future work will be also devoted to the following. To overcome the ill-posedness of the identification problem in the second step of the incremental approach one can add a (Tikhonov) regularization term to the corresponding objective functional, cf. [11]. So far, we did not sufficiently take into account the nonlinearity of the problem. Instead of the relatively simple CG method other iterative solution techniques for nonlinear

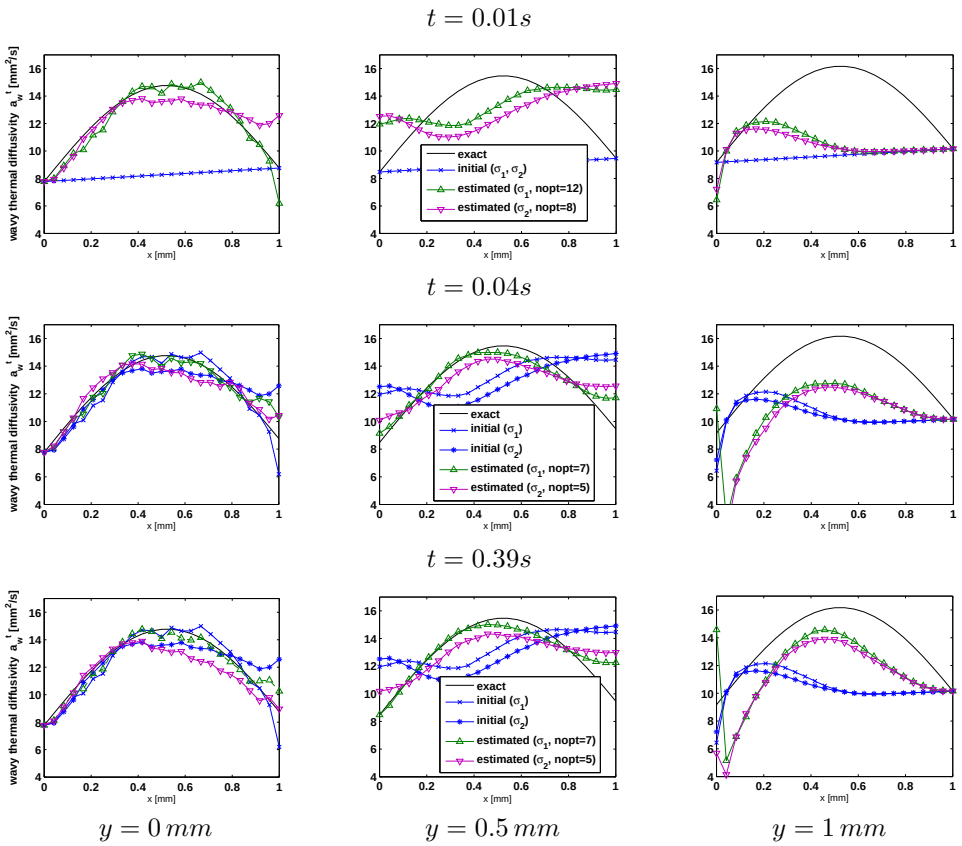


FIG. 4.13. *Estimated wavy thermal diffusivity $a_w^t$ for different noise levels of $\sigma_1$ and $\sigma_2$ after corresponding optimal nopt iterations at different times for constant $z = 0.5\,mm$ and different $y$.*

inverse problems, e. g. truncated Newton-CG [15], combined with a suitable line search strategy can be applied. A further issue is a better theoretical understanding of the error propagation through the sequence of inverse problems. Finally, in this paper we do not present a detailed comparison with simultaneous approaches (as, for another problem class, in [4]). Such a comparative study is a topic of current research.

**Acknowledgements.** The authors gratefully acknowledge the financial support of the Deutsche Forschungsgemeinschaft (DFG) within the Collaborative Research Center (SFB) 540 "Model-based experimental analysis of kinetic phenomena in fluid multiphase reactive systems".

REFERENCES

[1] O. M. ALIFANOV, *Inverse Heat Transfer Problems*, Springer, Berlin, 1994.

[2] O. M. ALIFANOV, E.A. ARTYUKHIN, AND S.V. RUMYANTSEV, *Extreme Methods for Solving Ill-Posed Problems with Applications to Inverse Heat Transfer Problems*, Begell House, Inc., U.S.A., 1995.

[3] O. M. ALIFANOV, Y. JARNY, P.V. PROSUNTSOV, AND G.A. IVANOV, *Complex identification of thermophysical properties of anisotropic composite material*, in Proceedings of the 5th international Conference on Inverse Problems in Engineering: Theory and Practice, Cambridge, U.K., 2005.

[4] A. Bardow and W. Marquardt, *Incremental and simultaneous identification of reaction kinetics: methods and comparison*, Chem. Eng. Sci., 59 (2003), pp. 2673–2684.
[5] ———, *Identification of diffusive transport by means of an incremental approach*, Comp. Chem. Eng., 28 (2004), pp. 585–595.
[6] H. Brauer, *Strömung und Wärmeübergang bei Rieselfilmen*, in VDI-Forsch.-Heft 457, VDI-Verlag, Düsseldorf, 1956.
[7] M. Brendel, D. Bonvin, and W. Marquardt, *Incremental identification of kinetic models for homogeneous reaction systems*, Chem. Eng. Sci., 61 (2006), pp. 5404–5420.
[8] R. S. Brodkey and H. C. Hershey, *Transport Phenomena — A Unified Approach*, McGraw-Hill Book Company, U.S.A, 1976.
[9] G. Dietze, V.V. Lel, and R. Kneer, *Modelling of heat transfer in stable wavy film flow based on effective thermal diffusivity*, in Proceedings of IHTC-13 2006, Sidney, 2006.
[10] *DROPS package*. `http://www.igpm.rwth-aachen.de/DROPS/`.
[11] H. W. Engl, M. Hanke, and A. Neubauer, *Regularization of Inverse Problems*, Kluwer Academic Publishers, Dordrecht, 1996.
[12] R. Fletcher and C. M. Reeves, *Function minimization by conjugate gradients*, J. Comput., 7 (1964), pp. 149–154.
[13] A. L. Frenkel and K. Indireshkumar, *Wavy film flows down an inclined plane: Perturbation theory and general evolution equation for the film thickness*, Phys. Rev. E, 60 (1999), pp. 4143–4157.
[14] S. Gross, M. Soemers, A. Mhamdi, F. Al Sibai, A. Reusken, W. Marquardt, and U. Renz, *Identification of boundary heat fluxes in a falling film experiment using high resolution temperature measurements*, Int. J. Heat Mass Tran., 48 (2005), pp. 5549–5562.
[15] M. Hanke, *Regularizing properties of a truncated Newton-CG algorithm for nonlinear inverse problems*.
[16] M. Hanke and O. Scherzer, *Error analysis of an equation error method for the identification of the diffusion coefficient in a quasi-linear parabolic differential equation*, SIAM J. Appl. Math., 59 (1999), pp. 1012–1027.
[17] C. Hansen, *Rank-Deficient and Discrete Ill-posed Problems: Numerical Aspects of Linear Inversion*, SIAM Monographs on Mathematical Modeling and Computation, SIAM, Philadelphia, 1998.
[18] J. C. Marcelo, G. S. Dulikravich, H.R. Orlande, and A. F. Rodrigues, *A comparison of two solution techniques for the inverse problem of simultaneously estimating the spatial variations of diffusion coefficient and source terms*, in Proceedings of IMECE'03, 2003 ASME International Mechanical Engineering Congress and Exposition, Washington, D.C., U.S.A., 2003.
[19] W. Marquardt, *Towards a process modeling methodology*, R. Berber (Ed.), Methods of Model-Based Control, (1995), pp. 3–41.
[20] ———, *Model-based experimental analysis of kinetic phenomena in multi-phase reactive systems*, Chem. Eng. Res. Des., 83 (2005), pp. 561–573.
[21] J. Nocedal and S. J. Wright, *Numerical Optimization*, Springer Series in Operations Research, Springer, Berlin, Heidelberg, New York, 1999.
[22] M.K. Panga, R. R. Mudunuri, and V. Balakotaiah, *Long-wavelength equation for vertically falling films*, Phys. Rev. E, 71 (2005), p. 036310 (18 pages).
[23] L. Prandtl, *ber Flssigkeitsbewegung bei sehr kleiner Reibung*, in Gesammelte Abhandlungen zur angewandten Mechanik, Hydro- und Aerodynamik, W. Tolmien, H. Schlichting, and H. Grtler, eds., vol. 2, Springer-Verlag, Berlin, 1961, ch. 4.
[24] G.R. Richter, *Numerical identification of a spatially varying diffusion coefficient*, Math. Comput., 36 (1981), pp. 375–386.
[25] Y. Saad, *Iterative Methods for Sparse Linear Systems*, SIAM, Philadelphia, PA, USA, 2003.
[26] J. Su and F. H. Geoffrey, *Inverse heat conduction problem of estimating time-varying heat transfer coefficient*, Numer. Heat Transf., 45 (2004), pp. 777–789.
[27] E. Walter and L. Pronzato, *Identification of Parametric Models from Experimantal Data*, Springer, Berlin, 1997.
[28] W. Wilke, *Wärmeübergang an Rieselfilmen*, in VDI-Forsch.-Heft 490, VDI-Verlag, Düsseldorf, 1962.